

# Model reduction for the collective dynamics of globally coupled oscillators

Lachlan D. Smith<sup>1,\*</sup> and Georg A. Gottwald<sup>1,†</sup>

<sup>1</sup>*School of Mathematics and Statistics, The University of Sydney, Sydney, NSW 2006, Australia*

(Dated: October 2, 2019)

Model reduction techniques such as the Ott-Antonsen ansatz have been widely used to study the collective behavior of globally coupled oscillators. However, the Ott-Antonsen approach assumes that there are infinitely many oscillators. Here we propose a new ansatz, based on a collective coordinate approach, that more accurately reproduces the collective dynamics of the Kuramoto model for finite networks, and yields the same dynamics as the Ott-Antonsen approach in the limit of infinitely many oscillators.

## I. INTRODUCTION

Many natural phenomena and industry applications can be modeled as networks of coupled oscillators, including firefly flashing [1], neuron firing [2, 3], and power grid dynamics [4]. A common phenomenon in networks of coupled oscillators is synchronization. Model reduction techniques aim to understand and quantify this low-dimensional emergent macroscopic dynamics. For the Kuramoto model [5–12], which is widely used to model networks of coupled oscillators, Ott and Antonsen [13] introduced a method that describes its low-dimensional dynamics. Many studies have since applied and generalized the Ott-Antonsen approach to describe low-dimensional phenomena such as chimera states [14–16], cluster synchronization from higher order coupling [17] or symplectic coupling [18], chaotic intercluster dynamics [19], and hysteretic synchronization [20]. However, the Ott-Antonsen approach assumes that there are infinitely many oscillators. Another commonly used model reduction approach is Watanabe-Strogatz theory [21] which is not restricted to the thermodynamic limit of infinitely many oscillators, but only applies to populations of identical oscillators [22].

Here we propose a new ansatz, based on the collective coordinate approach [23–26], that accurately describes the macroscopic dynamics of the Kuramoto model. We will show that, unlike the Ott-Antonsen ansatz, the collective coordinate approach quantitatively captures the macroscopic dynamics for finite populations of oscillators. For finite networks, both the new collective coordinate ansatz and the previous collective coordinate ansatz [23–26] (which is based on a linearization) better reproduce the collective dynamics compared to the Ott-Antonsen ansatz, with the new collective coordinate ansatz yielding a significant improvement compared to both previous methods. We will also show that the new collective coordinate ansatz yields identical macroscopic dynamics as the Ott-Antonsen ansatz in the thermodynamic limit of infinitely many oscillators, recovering well-known conditions for partial synchronization.

The paper is organized as follows. In Section II the collective coordinate framework for model reduction is described and the new ansatz is presented. In Section III numerical and analytical results are presented for finite networks with several natural frequency distributions. In Section IV the thermodynamic limit is studied. Section V summarizes the results.

## II. COLLECTIVE COORDINATE REDUCTION FOR FINITE NETWORKS

For a network of  $N$  coupled oscillators, each with phase  $\phi_i$ , the Kuramoto model [5] with all-to-all coupling is given by

$$\dot{\phi}_i = \omega_i + \frac{K}{N} \sum_{j=1}^N \sin(\phi_j - \phi_i), \quad (1)$$

where the natural frequencies  $\omega_i$  have distribution  $g(\omega)$  and  $K$  is the coupling strength.

The general method of collective coordinates is to assume some ansatz for the synchronized state, i.e.  $\phi_i \approx \hat{\phi}_i(\alpha)$  for  $i \in \mathcal{C}$ , where  $\mathcal{C}$  is the set of oscillators that synchronize, and the parameter  $\alpha(t)$  controls the shape of the synchronized state. The error incurred by this ansatz is given by substituting the ansatz into (1),

$$\mathcal{E}_i = \dot{\alpha} \frac{d\hat{\phi}_i}{d\alpha} - \omega_i - \frac{K}{N} \sum_{j \in \mathcal{C}} \sin(\hat{\phi}_j - \hat{\phi}_i),$$

for  $i \in \mathcal{C}$ . We ignore “rogue” oscillators with  $i \notin \mathcal{C}$  that do not synchronize. These rogue oscillators have no effect on the synchronized cluster in the thermodynamic limit, and this effect is assumed to be negligible for finite  $N$ . Since we are assuming a solution to the Kuramoto model (1) of the form  $\phi = \hat{\phi}(\alpha)$ , the error vector  $\mathcal{E}$  is minimized provided that it is orthogonal to the tangent space of the synchronization manifold spanned by  $\frac{d\hat{\phi}}{d\alpha}$ . The condition that  $\langle \mathcal{E}, \frac{d\hat{\phi}}{d\alpha} \rangle = 0$  provides the evolution equation for the collective coordinate variable

$$\dot{\alpha} = \frac{1}{\| \frac{d\hat{\phi}}{d\alpha} \|^2} \left( \left\langle \omega, \frac{d\hat{\phi}}{d\alpha} \right\rangle + \frac{K}{N} \sum_{i,j \in \mathcal{C}} \frac{d\hat{\phi}_i}{d\alpha} \sin(\hat{\phi}_j - \hat{\phi}_i) \right). \quad (2)$$

\* lachlan.smith@sydney.edu.au

† georg.gottwald@sydney.edu.au

A stable stationary point  $\alpha^*$  of (2) corresponds to a synchronized state  $\phi_i = \hat{\phi}_i(\alpha^*)$ , for  $i \in \mathcal{C}$ . The set  $\mathcal{C}$  is defined as the maximal set of oscillators such that stationary points of (2) exist.

To motivate the choice of  $\hat{\phi}$ , we introduce the complex order parameter

$$z(t) = r(t)e^{i\psi(t)} = \frac{1}{N} \sum_j e^{i\phi_j}.$$

The Kuramoto model (1) can be rewritten as a mean-field equation

$$\dot{\phi}_i = \omega_i + Kr \sin(\psi - \phi_i), \quad (3)$$

where we have assumed, without loss of generality, that the mean natural frequency is zero. Similarly, we can assume that  $\psi = 0$ . In the partially synchronized state, oscillators in  $\mathcal{C}$  become approximately stationary, so that

$$\phi_i \approx \arcsin\left(\frac{\omega_i}{K\bar{r}}\right), \quad (4)$$

where

$$\bar{r} = \lim_{T \rightarrow \infty} \frac{1}{T} \int_0^T r(t) dt, \quad (5)$$

is the time-averaged order parameter. For large  $K$ , (4) can be expanded to obtain  $\phi_i \approx \frac{\omega_i}{K\bar{r}} + \mathcal{O}(K^{-3})$ , which motivates the choice of ansatz

$$\hat{\phi}_i = \alpha \omega_i, \quad (6)$$

used in previous studies [23–26]. Note that  $\alpha \sim 1/(K\bar{r})$ . We refer to (6) as the *linear* collective coordinate ansatz. As a new ansatz, we choose  $\alpha = \bar{r}$  as the collective coordinate and write (4) as

$$\hat{\phi}_i = \arcsin\left(\frac{\omega_i}{K\alpha}\right). \quad (7)$$

We refer to (7) as the *arcsin* collective coordinate ansatz. For this new ansatz (7), the evolution equation for the collective coordinate (2) becomes

$$\frac{d\hat{\phi}}{d\alpha} \dot{\alpha} = - \left( \sum_{i \in \mathcal{C}} \frac{s_i^2}{\sqrt{1-s_i^2}} \right) \left[ 1 - \frac{1}{N\alpha} \sum_{j \in \mathcal{C}} \sqrt{1-s_j^2} \right], \quad (8)$$

where  $s_i = \frac{\omega_i}{K\alpha}$ . The sum in round brackets in (8) is positive provided that  $|\mathcal{C}| > 1$ , i.e., there is a non-trivial cluster, and stationary points of the evolution equation (8) correspond to solutions to

$$1 = \frac{1}{N\alpha} \sum_{j \in \mathcal{C}} \sqrt{1-s_j^2}, \quad (9)$$

which only has a single sum, compared to the double sum in (2).

For the linear ansatz (6), and a set of oscillators  $\mathcal{C}$ , stationary points of (2), if they exist, always form a pair (one stable and one unstable) which annihilate via a saddle-node bifurcation at  $K = K_1(\mathcal{C})$  [23]. For the arcsin ansatz (7) the bifurcation sequence is more complex, with saddle-node bifurcations occurring at values  $K_1(\mathcal{C})$  and  $K_2(\mathcal{C}) > K_1$ . For  $K > K_2(\mathcal{C})$  there exists a single stationary point of (2), which is stable. Upon decreasing  $K$ , at  $K = K_2(\mathcal{C})$  a pair of stationary points emerge via a saddle-node bifurcation, one real and unstable, the other with non-zero imaginary part and stable. Decreasing  $K$  further, the two real stationary points coalesce and split off the real axis in a saddle-node bifurcation at  $K = K_1(\mathcal{C})$ , leaving only imaginary stationary points, which have no physical meaning. This bifurcation sequence is explained in more detail in Appendix A. For both collective coordinate ansatzes, stable stationary points of (2) may be found for  $K < K_1(\mathcal{C})$  for smaller subsets  $\mathcal{C}' \subset \mathcal{C}$ , and the bifurcation sequence repeats. Therefore, for both collective coordinate ansatzes, the transition from global synchronization to partial synchronization, and then to incoherence, as  $K$  decreases, occurs for unimodal frequency distributions as a cascade of saddle-node bifurcations, successively removing more and more oscillators from the synchronized set  $\mathcal{C}$ . This is consistent with the onset of synchronization being a second order phase transition for unimodal frequency distributions.

The collective coordinate solution  $\hat{\phi}(\alpha^*)$  allows us to express the order parameter as

$$\bar{r}_{CC} = \frac{1}{N} \left| \sum_{j \in \mathcal{C}} e^{i\hat{\phi}_j(\alpha^*)} \right|. \quad (10)$$

For the arcsin collective coordinate ansatz (7), the collective coordinate  $\alpha$  replaces  $\bar{r}$  in the mean field solution (4). Therefore, instead of computing  $\bar{r}_{CC}$  using (10), we could compute  $\bar{r}_{CC} = \alpha^*$ . We show in Appendix B that the two methods for computing  $\bar{r}_{CC}$  are equivalent, that is,  $\alpha^* = \bar{r}_{CC}$  as computed using (10). This means that the arcsin collective coordinate ansatz is self-consistent, which is not true for the linear collective coordinate ansatz.

We will show in the following section that the new arcsin ansatz yields significantly better approximations of the macroscopic dynamics of (1) than both the original collective coordinate ansatz (6) and the Ott-Antonsen ansatz.

### III. PERFORMANCE OF THE COLLECTIVE COORDINATE FRAMEWORK FOR FINITE NETWORKS

We quantify the accuracy of the respective model reduction methods by analyzing the differences between the order parameter  $\bar{r}$  obtained from the full Kuramoto model (5) and that obtained from the respective model reductions for several natural frequency distributions.

### A. Lorentzian natural frequencies

We first consider a Lorentzian natural frequency distribution

$$g(\omega) = \Delta [\pi(\omega^2 + \Delta^2)]^{-1}, \quad (11)$$

which is centered at zero and has spread  $\Delta > 0$ . In all simulations we choose  $\Delta = 1$ . Under the assumption of infinitely many oscillators, the Ott-Antonsen ansatz [13] yields the order parameter

$$\bar{r}_{\text{OA}} = \begin{cases} 0 & \text{if } K < 2\Delta \\ \sqrt{1 - \frac{2\Delta}{K}} & \text{if } K \geq 2\Delta \end{cases}. \quad (12)$$

#### 1. Equiprobable draw of natural frequencies

We first consider equiprobably drawn natural frequencies to control finite size effects and to mimic the thermodynamic limit for finite but large  $N$  [27]. Fig. 1(a) shows  $\bar{r}_{\text{KM}}$  for the full Kuramoto model (1) with a small ( $N = 50$ , closed circles) and a larger ( $N = 500$ , open circles) number of oscillators. At  $K_c \approx 2$  there is a second order transition from the incoherent state, with  $\bar{r}_{\text{KM}} \sim \mathcal{O}(1/\sqrt{N})$ , to a partially synchronized state. The order parameter curves for  $N = 50$  and  $N = 500$  are very similar, albeit the curve for  $N = 500$  is smoother as it more closely represents the thermodynamic limit. The differences between  $\bar{r}_{\text{CC}}$  and  $\bar{r}_{\text{KM}}$  obtained from the full Kuramoto model (1) with  $N = 50$  and  $N = 500$  are shown in Fig. 1(b) and Fig. 1(c), respectively, for the linear collective coordinate ansatz (6) and the arcsin collective coordinate ansatz (7), as well as the difference between  $\bar{r}_{\text{OA}}$  (12) and  $\bar{r}_{\text{KM}}$ . The differences are shown for  $K > K_c \approx 2$ , such that a synchronized cluster of oscillators exists. For  $N = 50$  (Fig. 1(b)), the arcsin ansatz (7) gives the best approximation for  $\bar{r}$ , and both collective coordinate ansatzes better reproduce  $\bar{r}$  compared to the Ott-Antonsen ansatz. For  $N = 500$  (Fig. 1(c)), the linear collective coordinate ansatz (6) does not perform as well as either the Ott-Antonsen ansatz or the arcsin collective coordinate ansatz (7), both of which accurately reproduce  $\bar{r}$ . The arcsin collective coordinate ansatz still yields the best approximation for  $\bar{r}$ , by a factor of at least 2 for  $K \geq 3$ . We note that both the Ott-Antonsen ansatz and arcsin collective coordinate ansatz generally yield smaller values for  $\bar{r}$  compared to the full Kuramoto model, whereas the linear collective coordinate ansatz generally yields greater values for  $\bar{r}$  compared to the full Kuramoto model.

#### 2. Random draw of natural frequencies

We now show that the collective coordinate method accurately captures the macroscopic dynamics when the natural frequencies are drawn randomly and finite size

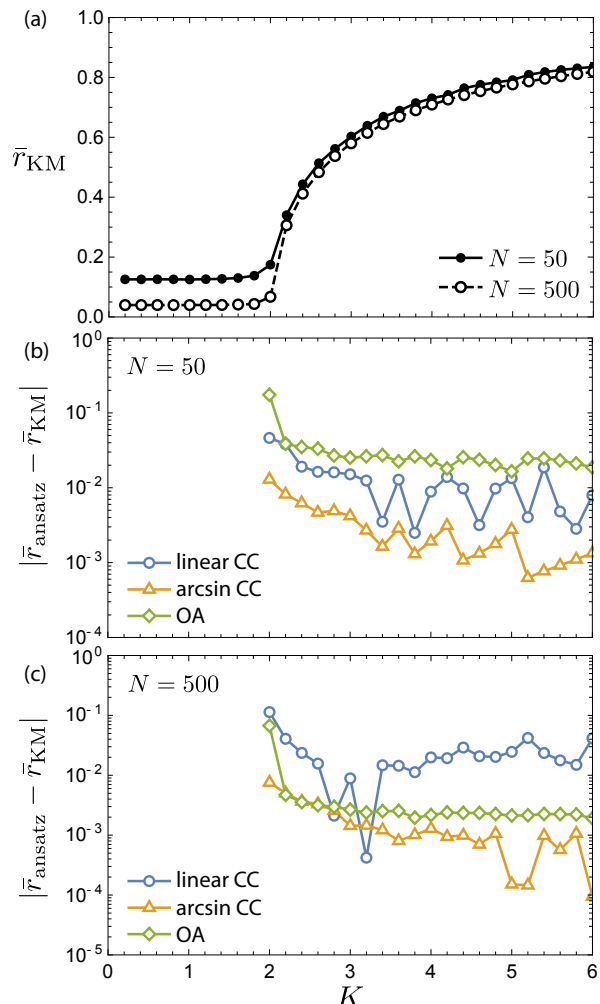


FIG. 1. (a) Time-averaged order parameter  $\bar{r}_{\text{KM}}$  for the Kuramoto model (1) with  $N = 50$  (closed circles) and  $N = 500$  (open circles) oscillators with equiprobably drawn Lorentzian distributed natural frequencies (11) with  $\Delta = 1$ . (b,c) Difference between  $\bar{r}_{\text{KM}}$  obtained from the full Kuramoto model [(b)  $N = 50$ , (c)  $N = 500$ ] and  $\bar{r}_{\text{ansatz}}$  obtained from the collective coordinate approaches (10) and the Ott-Antonsen approach (12) (green diamonds). For the collective coordinate approaches results are shown for the linear ansatz (6) (blue circles) and the arcsin ansatz (7) (orange triangles). The differences are shown for  $K > K_c$ , when a synchronized cluster exists.

effects become exacerbated. Fig. 2(a) shows  $\bar{r}_{\text{KM}}$  for the full Kuramoto model (1) with  $N = 50$  oscillators with randomly drawn Lorentzian distributed frequencies. Compared to equiprobably drawn frequencies (Fig. 1(a)), the transition from the incoherent state to the partially synchronized state is not as well defined for randomly drawn frequencies (Fig. 2(a)). This is due to the existence of small synchronized clusters which gradually merge as  $K$  increases. The error in reproducing the order parameter  $\bar{r}_{\text{KM}}$  is shown in Fig. 2(b) for the collective coordinate ansatzes and the Ott-Antonsen ansatz. The differences in  $\bar{r}$  are shown for values  $K \geq 2.2$ , such that there exists

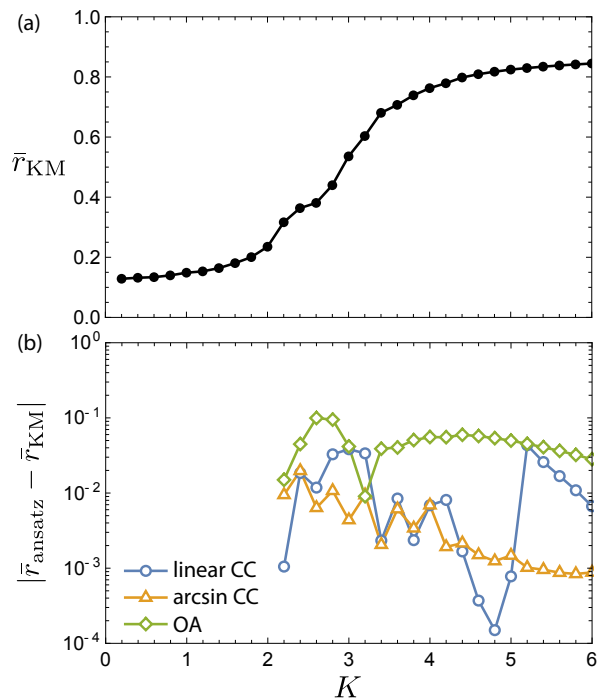


FIG. 2. (a) Time averaged order parameter  $\bar{r}_{KM}$  for the Kuramoto model (1) with  $N = 50$  oscillators with randomly drawn Lorentzian distributed natural frequencies (11) with  $\Delta = 1$ . (b) Difference between  $\bar{r}_{KM}$  obtained from the full Kuramoto model and  $\bar{r}_{ansatz}$  obtained from the collective coordinate approaches (10) and the Ott-Antonsen approach (12) (green diamonds). For the collective coordinate approaches results are shown for the linear ansatz (6) (blue circles) and the arcsin ansatz (7) (orange triangles). The differences are shown for  $K \geq 2.2$ , when a synchronized cluster with at least 10 oscillators exists.

a synchronized cluster with at least 10 oscillators. For smaller values of  $K$  there are small synchronized clusters consisting of only a few oscillators, whose dynamics can be approximated by a more complex collective coordinate ansatz [23, 25, 26]. We again see that the arcsin collective coordinate ansatz provides the best prediction for  $\bar{r}$ , and the Ott-Antonsen ansatz generally gives the worst prediction. This is not surprising since the natural frequencies are far from the thermodynamic limit assumption made by the Ott-Antonsen approach.

Along with accurately predicting  $\bar{r}$ , the collective coordinate approach also has the advantage of being able to predict the set of oscillators  $\mathcal{C}$  that will synchronize. We show in Appendix C that the arcsin collective coordinate ansatz generally predicts  $\mathcal{C}$  exactly compared to the full Kuramoto model, whereas the linear collective coordinate ansatz generally over-predicts the size of the cluster.

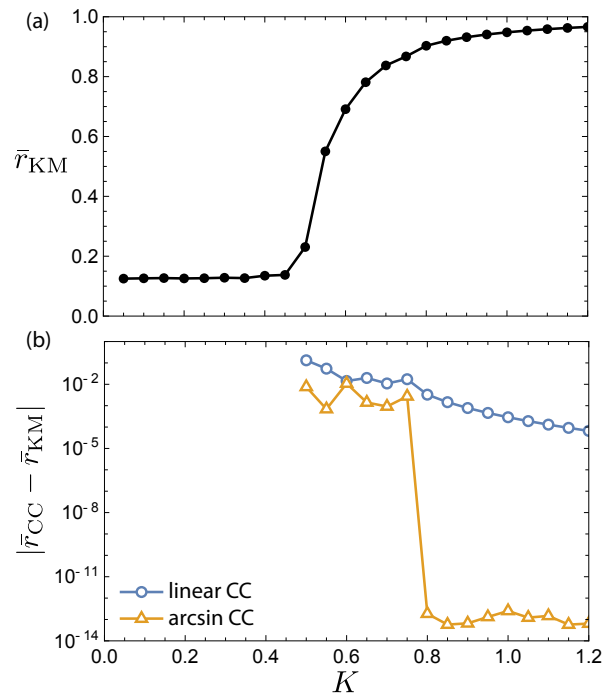


FIG. 3. (a) Time averaged order parameter  $\bar{r}_{KM}$  for the Kuramoto model (1) with  $N = 50$  oscillators with equiprobable Gaussian distributed natural frequencies (mean zero, and variance  $\sigma^2 = 0.1$ ). (b) Difference between  $\bar{r}_{KM}$  obtained from the full Kuramoto model (5) and  $\bar{r}_{CC}$  obtained from collective coordinate ansatzes (10). Results are shown for the linear ansatz (6) (blue circles) and the arcsin ansatz (7) (orange triangles). The differences are shown for  $K \geq 0.5$ , when a synchronized cluster exists.

## B. General natural frequency distributions

We now consider more general natural frequency distributions such as Gaussian and uniform distributions. The efficacy of the linear collective coordinate ansatz (6) has previously been demonstrated for unimodal and multimodal Gaussian distributions and for uniform distributions [23–26]. We show in Fig. 3 and Fig. 4 that the arcsin collective coordinate ansatz (7) yields an improved estimate for  $\bar{r}$  compared to the linear collective coordinate ansatz (6) also for Gaussian and uniformly distributed natural frequencies. In fact, for values of  $K$  such that all  $N$  oscillators synchronize ( $K \geq 0.8$  for the Gaussian case and  $K \geq 1.3$  for the uniform case) we find that the difference between  $\bar{r}_{CC}$  obtained from the arcsin collective coordinate approach compared to  $\bar{r}_{KM}$  obtained from the full Kuramoto model (5) is  $\mathcal{O}(10^{-13})$ , which suggests that the arcsin collective coordinate method is exact when all oscillators synchronize. The small errors that we observe result from neglecting the “rogue” oscillators. A more complex ansatz could be used to better approximate the effect of the rogue oscillators on the synchronized cluster, providing an even better approximation for the dynamics.

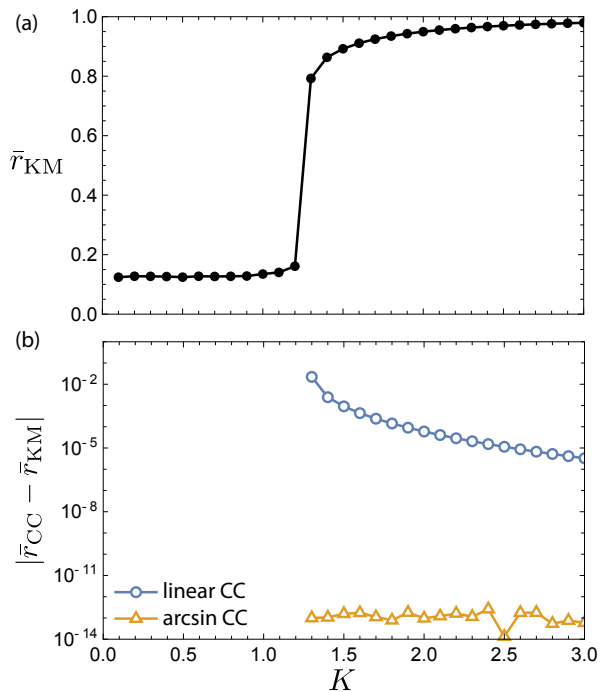


FIG. 4. (a) Time averaged order parameter  $\bar{r}_{\text{KM}}$  for the Kuramoto model (1) with  $N = 50$  oscillators with equiprobable uniformly distributed natural frequencies between  $-1$  and  $1$ . (b) Difference between  $\bar{r}_{\text{KM}}$  obtained from the full Kuramoto model (5) and  $\bar{r}_{\text{CC}}$  obtained from collective coordinate ansatzes (10). Results are shown for the linear ansatz (6) (blue circles) and the arcsin ansatz (7) (orange triangles). The differences are shown for  $K \geq 1.3$ , when a synchronized cluster exists.

#### IV. COLLECTIVE COORDINATE REDUCTION IN THE THERMODYNAMIC LIMIT

We now show analytically that the arcsin collective coordinate ansatz yields the same macroscopic dynamics as the Ott-Antonsen ansatz in the thermodynamic limit, and recovers well-known relations between the coupling strength and the order parameter for partially synchronized states. Taking the limit as  $N \rightarrow \infty$  in the evolution equation for the collective coordinate (2) involves replacing summations with integrals, i.e.,

$$\lim_{N \rightarrow \infty} \frac{1}{N} \sum_{i \in \mathcal{C}} h(\omega_i) \longrightarrow \int_{-\omega_{\mathcal{C}}}^{\omega_{\mathcal{C}}} h(\omega) g(\omega) d\omega,$$

for some function  $h$ , where  $\omega_{\mathcal{C}} = \lim_{N \rightarrow \infty} \max_{i \in \mathcal{C}} |\omega_i|$ . For the arcsin ansatz (7),  $\omega_{\mathcal{C}} \rightarrow K\alpha$  as  $N \rightarrow \infty$  (since the domain of arcsin is  $[-1, 1]$ ), and the evolution equation (2) becomes

$$I_3 \dot{\alpha} = I_1 + K I_2, \quad (13)$$

where

$$\begin{aligned} I_1 &= \lim_{N \rightarrow \infty} \frac{1}{N} \left\langle \omega, \frac{d\hat{\phi}}{d\alpha} \right\rangle \\ I_2 &= \lim_{N \rightarrow \infty} \frac{1}{N^2} \sum_{i, j \in \mathcal{C}} \frac{d\hat{\phi}_i}{d\alpha} \sin(\hat{\phi}_j - \hat{\phi}_i) \\ I_3 &= \lim_{N \rightarrow \infty} \frac{1}{N} \left\langle \frac{d\hat{\phi}}{d\alpha}, \frac{d\hat{\phi}}{d\alpha} \right\rangle. \end{aligned}$$

Replacing  $\alpha$  with  $r$ , (13) can be expanded to yield

$$\begin{aligned} I_3 \dot{r} &= \int_{-Kr}^{Kr} g(\omega) \frac{d\hat{\phi}}{dr} \omega \times \\ &\quad \left[ 1 + \frac{K}{\omega} \int_{-Kr}^{Kr} g(\eta) \sin(\hat{\phi}(\eta) - \hat{\phi}(\omega)) d\eta \right] d\omega. \end{aligned} \quad (14)$$

Making the change of variables  $s = \frac{\omega}{Kr}$  and  $u = \frac{\eta}{Kr}$ , for the arcsin collective coordinate ansatz (7), equation (14) becomes

$$I_3 \dot{r} = -J_1(r, K) r (1 - J_2(r, K)), \quad (15)$$

where

$$J_1(r, K) = K^2 \int_{-1}^1 \frac{g(Krs)s^2}{\sqrt{1-s^2}} ds, \quad (16)$$

$$J_2(r, K) = K \int_{-1}^1 g(Kru) \sqrt{1-u^2} du. \quad (17)$$

Note that  $J_1 > 0$  provided that the synchronized set of oscillators (those satisfying  $|\omega| < Kr$ ) has non-zero measure. Stationary solutions  $r^*$  of (15) are given by  $r^* = 0$  and by solutions of

$$J_2(r^*, K) = 1. \quad (18)$$

This recovers the well-known condition for partial synchronization in the Kuramoto model in the thermodynamic limit (cf. eq. (4.5) in [6] and eq. (12) in [8]), which was also obtained via the Ott-Antonsen ansatz [28, 29].

For some natural frequency distributions the integrals (16) and (17) can be computed analytically. For example, for a Lorentzian distribution (11), the evolution equation (15) reduces to

$$\epsilon^{-1} \dot{r} = -2\Delta r + K (r - r^3), \quad (19)$$

where  $\epsilon = D/I_3$  with

$$D = \frac{\Delta}{E(\Delta + E)(Kr^2 + \Delta + E)} \text{ and } E = \sqrt{K^2 r^2 + \Delta^2}.$$

We note that in the limit as  $\omega_{\mathcal{C}} \rightarrow Kr$ , the integral  $I_3 \rightarrow \infty$ . This reflects the fact that there is critical slowing down  $\epsilon \rightarrow 0$  at the saddle-node bifurcation at

$K = \omega_C/r$ , such that synchronization of the oscillator with natural frequency  $\omega_C = Kr$  becomes unstable. Eq. (19) is exactly the evolution equation for  $r$  obtained via the Ott-Antonsen approach [13] on the time-scale  $\epsilon t$ . A pitchfork bifurcation occurs at  $K = 2\Delta$ , such that for  $K < 2\Delta$  the incoherent state ( $r = 0$ ) is stable, and for  $K > 2\Delta$  the incoherent state is unstable, and a stable synchronized state emerges, with  $r$  given by (12). Recall that we found in Section II that for finite networks the bifurcation from a partially synchronized state to the incoherent state is a saddle-node bifurcation. This is consistent with the thermodynamic limit experiencing a pitchfork bifurcation since pitchfork bifurcations are structurally unstable and transform into a saddle-node bifurcation upon a small perturbation.

For a uniform natural frequency distribution on the interval  $[-a, a]$ ,  $J_1 > 0$  for all  $K > 0$  and

$$J_2 = \begin{cases} \frac{\pi K}{4a} & \text{if } Kr \leq a \\ \frac{K}{2} \left( \frac{\sqrt{K^2 r^2 - a^2}}{K^2 r^2} + \frac{1}{a} \operatorname{arccsc} \left( \frac{Kr}{a} \right) \right) & \text{if } Kr > a \end{cases}$$

The transition to global synchronization occurs when  $\omega_C = Kr = a$  (cf. (7)). The condition (18) implies that this transition occurs at  $K_c = \frac{4a}{\pi}$ , and the order parameter at the transition is  $r_c = \pi/4$ , as was found previously [30]. Now, consider the possibility of partial synchronization, such that  $\dot{r} = 0$  and  $Kr < a$ . The condition (18) implies that  $K = \frac{4a}{\pi} = K_c$ , and so global synchronization occurs. Therefore, we can conclude that only global synchronization is possible, which recovers the well-known result that for uniform frequency distributions the transition to synchronization is a first-order “explosive” transition with  $r_c \neq 0$  [30].

For Gaussian natural frequency distributions the integrals (16) and (17) can be written in terms of modified Bessel functions of the first kind  $I_n(z)$ . For the Gaussian natural frequency distribution with mean zero and variance  $\sigma^2$  we obtain

$$J_2 = \frac{\sqrt{\pi} K \exp\left(-\frac{K^2 r^2}{4\sigma^2}\right)}{2\sqrt{2}\sigma} \left( I_0\left(\frac{K^2 r^2}{4\sigma^2}\right) + I_1\left(\frac{K^2 r^2}{4\sigma^2}\right) \right),$$

and the solutions to (18) give the stationary points  $r^*$ .

We remark that for the linear collective coordinate ansatz (6) analytic expressions for the evolution equation of the collective coordinate can also be obtained for uniform and Gaussian naturally frequency distributions [23].

## V. CONCLUSIONS

In summary, we have shown that for small numbers of oscillators the new collective coordinate ansatz (7) yields a significant improvement on the approximation of the macroscopic dynamics of the Kuramoto model, compared to the previously used collective coordinate ansatz (6) [23–26] and the Ott-Antonsen ansatz [13]. In addition,

in the thermodynamic limit of infinitely many oscillators the new collective coordinate ansatz (7) yields identical macroscopic dynamics as the Ott-Antonsen ansatz and recovers well-known relations between the order parameter and the coupling strength.

We note that since the arcsin collective coordinate ansatz (7) is based on the mean field formulation of the Kuramoto model (3), it is only applicable to networks of globally coupled oscillators. In contrast, the linear collective coordinate ansatz (6), which is based on a linearization of the Kuramoto model, can be applied to any network topology [25, 26]. As such, the linear collective coordinate ansatz is able to describe partial synchronization in the presence of topological clusters [25]. Both collective coordinate ansatzes can be generalized to consider frequency clustering, and the complex inter- and intra-cluster dynamics that result [23, 25, 26].

## ACKNOWLEDGMENTS

We wish to acknowledge support from the Australian Research Council, Grant No. DP180101991.

### Appendix A: Bifurcation analysis for the arcsin collective coordinate ansatz

According to eq. (9), for the arcsin collective coordinate ansatz (7), non-zero stationary points of the collective coordinate evolution equation (2) correspond to roots of

$$F_C(r, K) = -1 + \frac{1}{Nr} \sum_{j \in \mathcal{C}} \sqrt{1 - s_j^2},$$

where  $s_j = \omega_j/(Kr)$ . Fixing a set of oscillators  $\mathcal{C}$ ,  $F_C(r, K)$  is real provided that  $r > r_{\min} = \omega_C/K$ , where  $\omega_C = \max_{i \in \mathcal{C}} |\omega_i|$ . As an example, we consider  $N = 50$  oscillators with Lorentzian natural frequency distribution, such that the set  $\mathcal{C}$  consists of the 42 oscillators with natural frequencies closest to the mean frequency (which is zero). Fig. 5 shows the contours  $\operatorname{Re}(F_C) = 0$  (red) and  $\operatorname{Im}(F_C) = 0$  (blue) in the complex plane for four values of  $K$ . Roots of  $F_C$  correspond to intersections of the red and blue contours. In each plot we also show the dashed line  $\operatorname{Re}(r) = r_{\min} = \omega_C/K$ , such that for  $\operatorname{Re}(r) > r_{\min}$ ,  $\operatorname{Im}(F_C) = 0$  if and only if  $\operatorname{Im}(r) = 0$ . In particular, this means that real roots of  $F_C$  can only occur for  $\operatorname{Re}(r) > r_{\min}$ , i.e., to the right of the dashed vertical line. For large values of  $K$ ,  $F_C$  has a single real root  $r_1$ , as demonstrated in Fig. 5(d) for  $K = 4.245$ . Upon decreasing  $K$ , a second real root  $r_2$  emerges at a critical value  $K = K_2(\mathcal{C})$  which satisfies  $F_C(r_{\min}, K) = 0$ . For the example considered here we obtain  $K_2 = 4.2447$ . This second root is an unstable stationary point of the collective coordinate evolution equation (2). In the complex plane,  $r_2$  appears through a saddle-node bifurcation,

with a third root  $r_3$  emerging simultaneously satisfying  $\text{Re}(r_3) < r_{\min}$  and  $\text{Im}(r_3) < 0$ . The three roots can be observed in Fig. 5(b,c) for  $K = 4.2372$  and  $K = 4.24$  respectively. Decreasing  $K$  further,  $r_1$  decreases,  $r_2$  increases, and  $\text{Re}(r_3)$  decreases. At a second critical value,  $K = K_1(\mathcal{C})$ , the two real roots  $r_1$  and  $r_2$  coalesce, undergo a saddle-node bifurcation, and move off the real axis as a complex conjugate pair. This is shown in Fig. 5 for  $K = 4.237 < K_1 = 4.2371$ . The value of  $K_1(\mathcal{C})$  can be obtained by finding the value of  $K$  such that  $\max_{r \in \mathbb{R}} F_{\mathcal{C}}(r, K) = 0$ .

The bifurcation sequence for real  $r$  is summarized in Fig. 6. For  $K > K_2(\mathcal{C})$  there is a single stationary point, which is stable (solid). For  $K_1(\mathcal{C}) < K < K_2(\mathcal{C})$  there exist two stationary points, one stable (solid) and one unstable (dashed). At  $K = K_1(\mathcal{C})$  the two stationary points annihilate via a saddle-node bifurcation. For  $K < K_1(\mathcal{C})$ , there are no stationary points and the synchronized state of the set  $\mathcal{C}$  is unstable. There may still exist subsets  $\mathcal{C}' \subset \mathcal{C}$  such that  $F_{\mathcal{C}'}$  has real roots, yielding a smaller synchronized subset of oscillators. In the example shown, the cluster with the 40 oscillators with natural frequencies closest to zero form the maximal synchronized cluster

at  $K_1$ ; the two oscillators with largest natural frequencies are the ones that do not synchronize.

### Appendix B: Self-consistency of the arcsin collective coordinate ansatz

In this section we show that the arcsin collective coordinate ansatz (7) is self-consistent, in the sense that the two methods to obtain  $\bar{r}_{\text{CC}}$ , either  $\bar{r}_{\text{CC}} = \alpha^*$  or using equation (10), give identical results.

Suppose that  $\alpha^*$  is a stationary solution of (2), then

$$0 = \left\langle \omega, \frac{d\hat{\phi}}{d\alpha} \right\rangle + \frac{K}{N} \sum_{i,j \in \mathcal{C}} \frac{d\hat{\phi}_i}{d\alpha} \sin(\hat{\phi}_j - \hat{\phi}_i). \quad (\text{B1})$$

For the arcsin ansatz (7) we can compute

$$\frac{d\hat{\phi}_i}{d\alpha} = \frac{-\omega_i}{K\alpha^2 \sqrt{1 - \frac{\omega_i^2}{K^2\alpha^2}}},$$

and so (B1) becomes

$$0 = - \sum_{i \in \mathcal{C}} \frac{\omega_i^2}{K^2(\alpha^*)^2 \sqrt{1 - \frac{\omega_i^2}{K^2(\alpha^*)^2}}} - \frac{1}{N} \sum_{i,j \in \mathcal{C}} \frac{\omega_i}{K(\alpha^*)^2 \sqrt{1 - \frac{\omega_i^2}{K^2(\alpha^*)^2}}} \left[ \frac{\omega_j}{K\alpha^*} \sqrt{1 - \frac{\omega_i^2}{K^2(\alpha^*)^2}} - \frac{\omega_i}{K\alpha^*} \sqrt{1 - \frac{\omega_j^2}{K^2(\alpha^*)^2}} \right],$$

where we have divided both sides by  $K$ . Introducing  $\tilde{\omega}_i = \omega_i/(K\alpha^*)$  we can write

$$\begin{aligned} 0 &= - \sum_{i \in \mathcal{C}} \frac{\tilde{\omega}_i^2}{\sqrt{1 - \tilde{\omega}_i^2}} - \frac{1}{N\alpha^*} \sum_{i,j \in \mathcal{C}} \frac{\tilde{\omega}_i}{\sqrt{1 - \tilde{\omega}_i^2}} \left[ \tilde{\omega}_j \sqrt{1 - \tilde{\omega}_i^2} - \tilde{\omega}_i \sqrt{1 - \tilde{\omega}_j^2} \right] \\ &= - \sum_{i \in \mathcal{C}} \frac{\tilde{\omega}_i^2}{\sqrt{1 - \tilde{\omega}_i^2}} - \frac{1}{N\alpha^*} \sum_{i,j \in \mathcal{C}} \tilde{\omega}_i \tilde{\omega}_j - \frac{\tilde{\omega}_i^2}{\sqrt{1 - \tilde{\omega}_i^2}} \sqrt{1 - \tilde{\omega}_j^2} \\ &= - \sum_{i \in \mathcal{C}} \frac{\tilde{\omega}_i^2}{\sqrt{1 - \tilde{\omega}_i^2}} + \frac{1}{N\alpha^*} \left( \sum_{i \in \mathcal{C}} \frac{\tilde{\omega}_i^2}{\sqrt{1 - \tilde{\omega}_i^2}} \right) \left( \sum_{j \in \mathcal{C}} \sqrt{1 - \tilde{\omega}_j^2} \right), \end{aligned} \quad (\text{B2})$$

where we have assumed, without loss of generality, that  $\sum_{i \in \mathcal{C}} \omega_i = 0$ , which implies that  $\sum_{i,j \in \mathcal{C}} \tilde{\omega}_i \tilde{\omega}_j = 0$ . Rearranging (B2) yields

$$\begin{aligned} \alpha^* &= \frac{1}{N} \sum_{j \in \mathcal{C}} \sqrt{1 - \tilde{\omega}_j^2} \\ &= \frac{1}{N} \sum_{j \in \mathcal{C}} \sqrt{1 - \tilde{\omega}_j^2} + i\tilde{\omega}_j \\ &= \frac{1}{N} \sum_{j \in \mathcal{C}} \cos \left( \arcsin \left( \frac{\omega_j}{K\alpha^*} \right) \right) + i \sin \left( \arcsin \left( \frac{\omega_j}{K\alpha^*} \right) \right) \\ &= \frac{1}{N} \sum_{j \in \mathcal{C}} e^{i\hat{\phi}_j(\alpha^*)} = \bar{r}_{\text{CC}}. \end{aligned}$$

Therefore, we have shown that if  $\alpha^*$  is a stationary solution of (2), then  $\alpha^* = \bar{r}_{\text{CC}}$ , where  $\bar{r}_{\text{CC}}$  is computed using (10). Note that this self-consistency is true for any set of natural frequencies.

### Appendix C: Collective coordinate prediction of the synchronized cluster $\mathcal{C}$

The set of synchronized oscillators  $\mathcal{C}$  is predicted by the collective coordinate ansatzes as the maximal set of oscillators such that (2) has a stable stationary solution  $\alpha^*$ . The set  $\mathcal{C}$  can be found by starting at a high value of  $K$  such that most oscillators synchronize, and then suc-

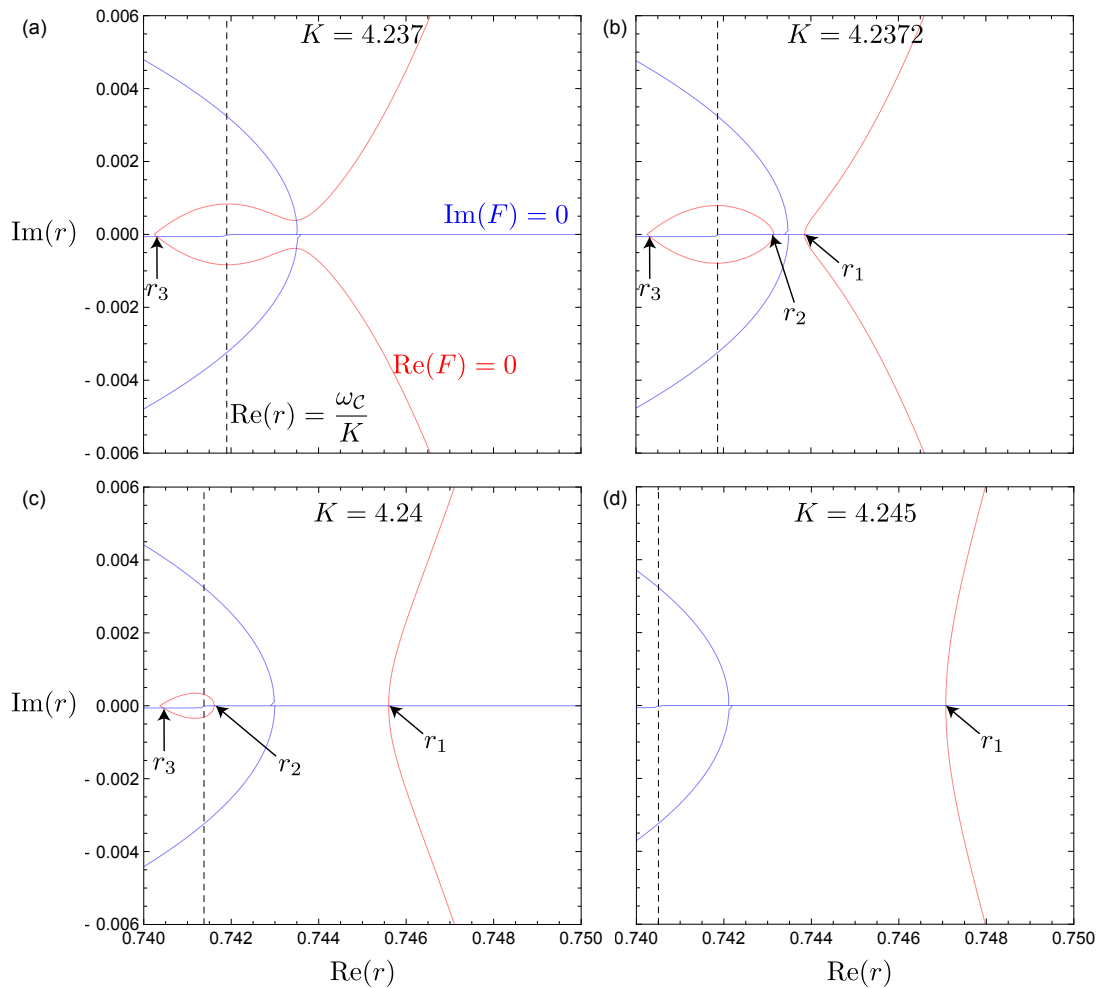


FIG. 5. Saddle-node bifurcations in the complex  $r$  plane for  $N = 50$  oscillators with Lorentzian natural frequency distribution, with the set  $\mathcal{C}$  consisting of the 42 oscillators with natural frequencies closest to the mean frequency. Stationary points of the collective coordinate evolution equation (2) correspond to intersections of the curves  $\text{Re}(F_{\mathcal{C}}) = 0$  (red) and  $\text{Im}(F_{\mathcal{C}}) = 0$  (blue). The line  $r = r_{\min} = \omega_{\mathcal{C}}/K$  is also shown for each  $K$ , such that for real  $r$ ,  $\text{Im}(F_{\mathcal{C}}) = 0$  if and only if  $r > r_{\min} = \omega_{\mathcal{C}}/K$ . (a) For  $K = 4.237$  there is a single root  $r_3$  of  $F_{\mathcal{C}}$ , which has non-zero imaginary part. (b,c) For  $K = 2.372, 4.24$  there are two roots,  $r_2$  and  $r_3$  of  $F_{\mathcal{C}}$ . (d) For  $K = 4.245$  there is only one root  $r_1$  of  $F_{\mathcal{C}}$ , which is real.

cessively removing oscillators from  $\mathcal{C}$  whenever stationary solutions of (2) cease to exist. For the full Kuramoto model (1) the set  $\mathcal{C}$  can be found by computing the effective frequency of each oscillator,

$$\bar{\omega}_i = \lim_{T \rightarrow \infty} \frac{1}{T} \int_0^T \dot{\phi}_i dt = \lim_{T \rightarrow \infty} \frac{\phi_i(T) - \phi_i(0) + 2\pi w_i(T)}{T},$$

where  $w_i(T) \in \mathbb{Z}$  is the winding number of the  $i$ -th oscillator. Synchronized clusters are sets of oscillators with the same effective frequency, and  $\mathcal{C}$  is the largest such synchronized cluster. Since we consider all-to-all coupling, if we label the oscillators in order of increasing natural frequencies, the synchronized cluster consists of all oscillators with indices between some minimum index

$C_{\min}$  and some maximum index  $C_{\max}$ . Hence, the size of the synchronized cluster is  $C_{\max} - C_{\min} + 1$ . Fig. 7 shows these lower ( $C_{\min}$ ) and upper ( $C_{\max}$ ) boundaries of the cluster for  $N = 50$  oscillators with randomly drawn Lorentzian distributed natural frequencies (the same as Fig. 2). As expected, the synchronized cluster grows in size monotonically upon increasing the coupling strength  $K$ , with the lower boundary  $C_{\min}$  decreasing monotonically and the upper boundary  $C_{\max}$  increasing monotonically. We observe that the arcsin collective coordinate ansatz (7) (orange triangles) agrees with the full Kuramoto model (solid black curve) for most values of  $K$ , whereas the linear collective coordinate ansatz (6) generally overpredicts the size of the synchronized cluster.

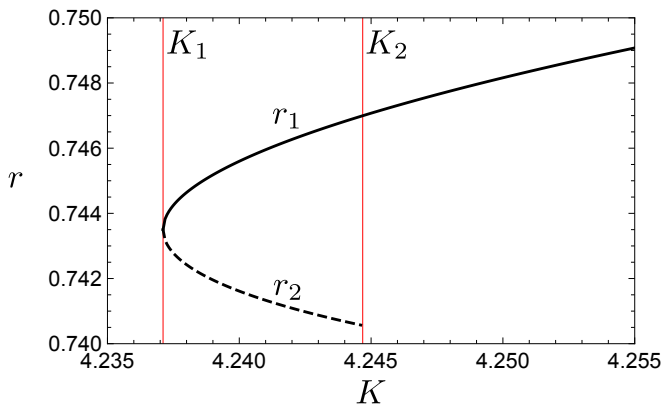


FIG. 6. Bifurcation sequence for real  $r$  corresponding to the plots shown in Fig. 5. For  $K > K_2$  there is a single real root  $r_1$ , which is a stable stationary point of the collective coordinate dynamics (2). Upon decreasing  $K$ , at  $K_2$  a second real root  $r_2$  emerges via a saddle-node bifurcation in the complex plane (cf. Fig. 5(c,d)). This root  $r_2$  is an unstable stationary point of the collective coordinate dynamics (2). At  $K = K_1$  the roots  $r_1$  and  $r_2$  annihilate via a saddle-node bifurcation (cf. Fig. 5(a,b)).

- 
- [1] R. Mirollo and S. Strogatz, *SIAM J. Appl. Math.* **50**, 1645 (1990).
- [2] J. H. Sheeba, A. Stefanovska, and P. V. E. McClintock, *Biophys. J.* **95**, 2722 (2008).
- [3] D. Bhowmik and M. Shanahan, in *The 2012 International Joint Conference on Neural Networks (IJCNN)* (2012) pp. 1–8.
- [4] G. Filatrella, A. H. Nielsen, and N. F. Pedersen, *Eur. Phys. J. B* **61**, 485 (2008).
- [5] Y. Kuramoto, *Chemical Oscillations, Waves, and Turbulence*, Springer Series in Synergetics, Vol. 19 (Springer-Verlag, Berlin, 1984) pp. viii+156.
- [6] S. H. Strogatz, *Physica D* **143**, 1 (2000).
- [7] A. Pikovsky, M. Rosenblum, and J. Kurths, *Synchronization: A Universal Concept in Nonlinear Sciences* (Cambridge University Press, Cambridge, 2001).
- [8] J. A. Acebrón, L. L. Bonilla, C. J. Pérez Vicente, F. Ritort, and R. Spigler, *Rev. Mod. Phys.* **77**, 137 (2005).
- [9] G. V. Osipov, J. Kurths, and C. Zhou, *Synchronization in Oscillatory Networks*, Springer Series in Synergetics (Springer, Berlin, 2007) p. 37c.
- [10] A. Arenas, A. Diaz-Guilera, J. Kurths, Y. Moreno, and C. Zhou, *Phys. Rep.* **469**, 93 (2008).
- [11] F. Dörfler and F. Bullo, *Automatica* **50**, 1539 (2014).
- [12] F. A. Rodrigues, T. K. D. Peron, P. Ji, and J. Kurths, *Phys. Rep.* **610**, 1 (2016).
- [13] E. Ott and T. M. Antonsen, *Chaos* **18**, 037113, 6 (2008).
- [14] M. J. Panaggio and D. M. Abrams, *Nonlinearity* **28**, R67 (2015).
- [15] C. R. Laing, *Chaos* **19**, 013113 (2009).
- [16] C. R. Laing, *Physica D* **238**, 1569 (2009).
- [17] P. S. Skardal, E. Ott, and J. G. Restrepo, *Phys. Rev. E* **84**, 036208 (2011).
- [18] P. S. Skardal and A. Arenas, *Phys. Rev. Lett.* **122**, 248301 (2019).
- [19] C. Bick, M. J. Panaggio, and E. A. Martens, *Chaos* **28**, 071102 (2018).
- [20] D. Pazó and E. Montbrió, *Phys. Rev. E* **80**, 046215 (2009).
- [21] S. Watanabe and S. H. Strogatz, *Phys. Rev. Lett.* **70**, 2391 (1993).
- [22] A. Pikovsky and M. Rosenblum, *Chaos* **25**, 097616 (2015).
- [23] G. A. Gottwald, *Chaos* **25**, 053111, 12 (2015).
- [24] G. A. Gottwald, *Chaos* **27**, 101103 (2017).
- [25] E. J. Hancock and G. A. Gottwald, *Phys. Rev. E* **98**, 012307 (2018).
- [26] L. D. Smith and G. A. Gottwald, *Chaos* **29**, 093127 (2019).
- [27] If  $G(\omega)$  denotes the cumulative distribution function of the frequencies, then  $G(\omega_i) = \frac{i}{N+1}$ , for  $i = 1, \dots, N$ .
- [28] O. E. Omel'chenko and M. Wolfrum, *Phys. Rev. Lett.* **109**, 164101 (2012).
- [29] O. E. Omel'chenko and M. Wolfrum, *Physica D* **263**, 74 (2013).
- [30] D. Pazó, *Phys. Rev. E* **72**, 046211, 6 (2005).

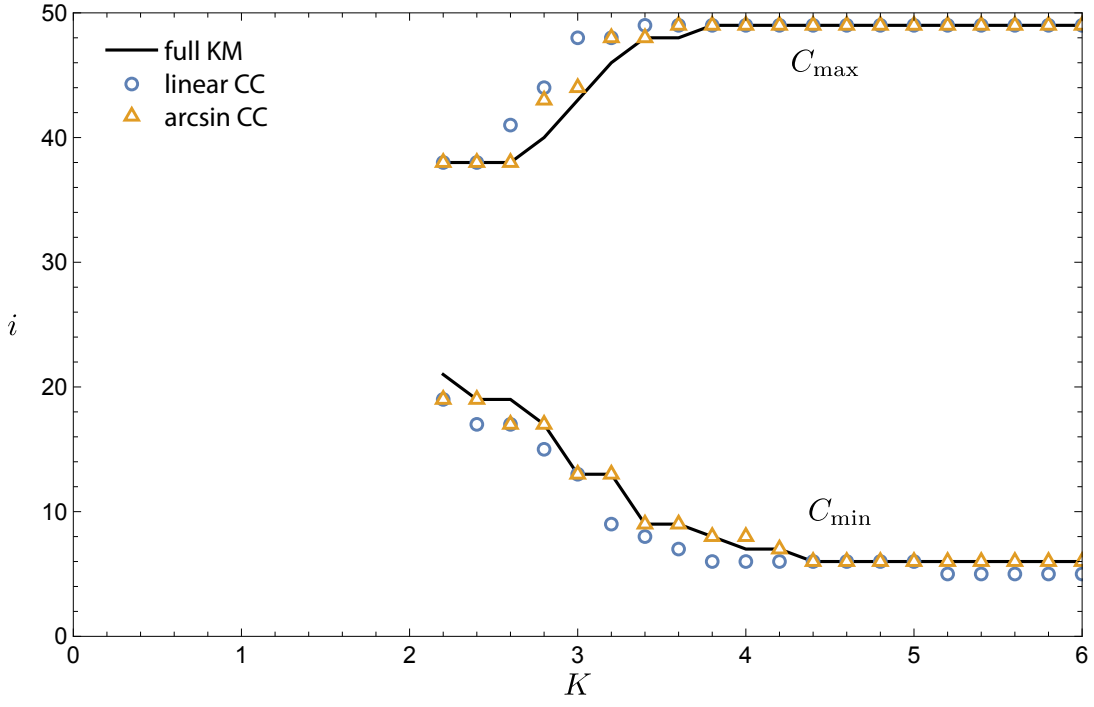


FIG. 7. Lower ( $C_{\min}$ ) and upper ( $C_{\max}$ ) boundaries of the synchronized cluster for  $N = 50$  oscillators with randomly drawn Lorentzian distributed natural frequencies (as in Fig. 2). Results are shown for the full Kuramoto model (solid black), and predictions using the linear collective coordinate ansatz (6) (blue circles) and the arcsin collective coordinate ansatz (7) (orange triangles), for  $K \geq 2.2$ , when a synchronized cluster with at least 10 oscillators exists.